MODELING STRESS AND DISTORTION OF FULL-FLOAT TRUCK AXLE DURING INDUCTION HARDENING PROCESS

Dr. Lynn Ferguson[(1)], Dr. Zhichao Li[(1)], Dr. Valentin Nemkov[(2)],
Robert Goldstein[(2)], John Jackowski[(2)], Greg Fett[(3)]

[(1)] Deformation Control Technology, Inc., 7261 Engle Rd., Suite 105, Cleveland, OH 44130 USA
[(2)] Fluxtrol, Inc., 1388 Atlantic Blvd., Auburn Hills, MI 48326 USA
[(3)] Dana Corporation, 3939 Technology Dr., Maumee, OH 43537 USA

ABSTRACT

Computer simulation of induction heat treating processes is relatively widespread within the industry. The bulk of the simulation studies considered coupling two of the multiple phenomena that occur during the process: 1) the electromagnetic and thermal process, and 2) the metallurgical and thermal-stress process. Recent studies have incorporated more of the mutually coupled phenomena into the simulation process. In these studies, electromagnetic, thermal, metallurgical, stress and shape change were coupled together using multiple programs. These studies enhanced our capabilities to predict the actual part performance of induction hardening process. This paper describes a study of a complex induction hardening process of a full-float truck axle. The process includes a dwell heating of the flange and a scan hardening of the shaft and spline. Computer simulation of electromagnetic and thermal processes was made using Flux software. The power densities from Flux are then exported and mapped into the DANTE for thermal, metallurgical, stress and distortion simulation. The study is based upon component test data from Dana Corporation.

INTRODUCTION

It is well known that changes in thermal distributions throughout an induction hardening process create complex layers of stresses in the component. Both residual stresses and mechanical properties of hardened pattern have significant impact on service performance of the heated treated parts. The induction hardening of steel components is a high nonlinear transient process, which is not intuitively understandable in general. With the development of FEA modelling capability in the past couple decades, both electro-magnetic and thermal stress analyses of the induction hardening have become more mature, and they have been successfully applied to understand and solve industrial problems [1]. The mechanical properties and residual stresses can be predicted by finite element analysis, which will further be used to analyse the mode and location of fatigue failures [2-5]. The component geometry and process can be also optimised to reduce part weight, manufacturing cost, and optimum performance.

When considering heat treatment of steel components, induction hardening is a common processing method due to its fast heating times, high efficiency, and ability to heat locally. However, predicting the final properties of a component after induction processing adds another

layer of complexity. Not only temperature and structure have to be considered, but also electromagnetism. When hardening of steel, the magnetic properties change throughout the process, affecting the thermal distribution and structure. Coupling these various phenomena to reach the end properties after treatment is a state of the art technology.

A simulation method is developed to use coil design and process settings combined with material and structure to calculate the post-process properties. This stage in the study focuses on the simulation steps needed to produce reliable results. Studies have been successfully accomplished for the development of simulation techniques for the prediction of electromagnetic and thermal effects, coupled with structural changes to predict a hardness pattern [6]. The recent drive is to go a step further for the inclusion of stress levels involved with thermally induced structural changes. This provides a more complete picture of the ultimate material properties. An investigation of stress and distortion modelling of a simple case of ID and OD hardening of a tubular product was previously studied and reported on [7]. It was next desired to perform a study on a component common in industry with a more complex geometry and subjected to external stresses in service. The case chosen for this study is a full-float truck axle with dimensions typical to those manufactured by Dana Corporation. Choosing an axle, being a common automotive component, allows for a comparison of simulation results to desired axle properties. The results are discussed in comparison to typical performance criteria for the case chosen. The ultimate goal of this continuous study is to produce results representative of actual part performance.

SELECTION OF CASE STUDY

Axles must be surface hardened for durability to prevent failure in service. The hardening process is commonly performed by induction scanning. How the induction scan process is performed affects the induced stresses and distortion. During induction hardening of truck axles with shaft length over 1 meter, the main concerns are the bowing distortion and the amount of growth in length. The bowing distortion can be minimized by proper inductor design, high quality process controls and structural support mechanisms. Excessive heat internal to the shaft is the main contributor to this problem, which can be evaluated by simulation. Change in length is affected by both heating and cooling rates of the shaft, and this is again a nonlinear process. A full-float truck axle from Dana Corporation is selected in this study. A simplified CAD model is shown in Figure 1. The length of the shaft is about 1008 mm; the fillet radius between the flange and the shaft is 9.52 mm; and diameter of the shaft is 34.93 mm; the thickness of the flange is 16.5 mm, and its diameter is 104.5 mm; the spline has 35 teeth in total.
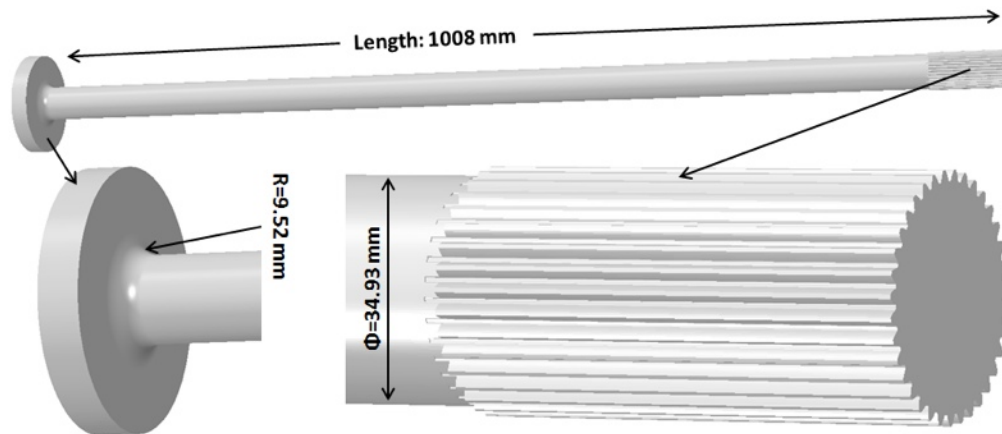
Figure 1: CAD model and brief geometry of the selected full-float truck axle.

The axle is made of AISI 1541, and its nominal chemical composition is used in this study. During cooling process after induction heating, phase transformations are involved. The austenite can transform to ferrite, pearlite, bainite, or martensite depending on the cooling rate. Accurate descriptions of phase transformations and mechanical properties of individual phases are required for thermal stress analysis [8].

DESIGN AND PROCESS CONSIDERATIONS

It is critical not only to meet the hardened depth requirement, but also prevent excessive heating in such areas as the flange, the core of the shaft, and edge of the spline. Too much heat in these regions is known to increase the cracking possibility, and lead to excessive distortion. The minimum case depth requirement for the shaft of this axle is 5.4 mm, and the case depth is defined by 40 HRC.

The inductor needs to be designed carefully to prevent cracking possibility and excessive distortion issues. A machined two-turn coil with magnetic flux concentrator was chosen and configured using Flux 2D. An example of a fully assembled coil of this style is displayed in Figure 2(a). The view is from the bottom of the coil. Inductor optimization steps were followed [7]. The bottom turn is profiled to help drive heat in the radius. The profile design is guided by providing the most amount of heat in the radius, while preventing a bulged pattern in the base of the shaft or on the flange. Flux concentrator Fluxtrol A® was applied to the bottom turn to further help drive heat into the radius and partially shield flux from coupling with the shaft to prevent a bulged pattern. The top turn is needed to aid in the scan process by widening the heat zone on the shaft. This allows for a faster scan speed. In Figure 2(a), the green material is Fluxtrol A®, surrounded by a grey quench body assembly. A quench body is mounted to the coil, which sprays quenchant about one inch below the coil. The quench is described in Flux by a heat transfer coefficient. A heat transfer coefficient of 25000 W/m²/k is used to represent the aggressive spray impact of 6% polymer solution. The quench follows at a location one inch below the coil as the coil scans up the shaft at 8 mm/s. A finite element meshing used to model the axle by Flux 2D is shown in Figure 2(b), with a schematic temperature distribution focusing on the flange and the fillet regions.
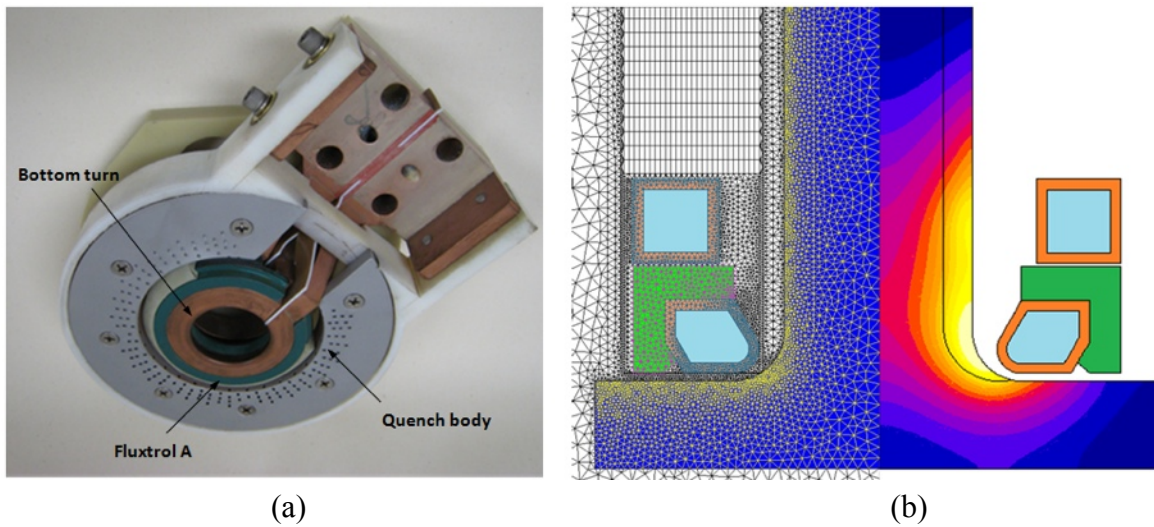
| (a) | (b) |

Figure 2: (a) Full assembly of a two-turn axle scan coil with quench body,
(b) Fillet area of axle modelled with Flux 2D, mesh elements

The material of the axle is magnetic, and the power density distribution varies greatly as the temperature exceeds the Curie point. The inductor frequency is 10 kHz, which is the common operating frequency of the Dana induction machines for this class of parts. The difference in skin effect can be seen easily during the scan of the shaft. The portion of the shaft above the bottom turn has high skin effect since it is under the Curie point. The bottom turn provides more intensive heating which drives the case depth and results in a deeper penetration of power at its heat face. Specifically when to turn off power at the end of the process can be calculated in Flux 2D by determining the temperature profile as the coil approaches the edge of the spline. Three snapshots of power distribution predicted by Flux 2D are shown in Figure 3. In these three snapshots, the inductor delivers power to the flange/fillet, the shaft, and the spline, respectively.
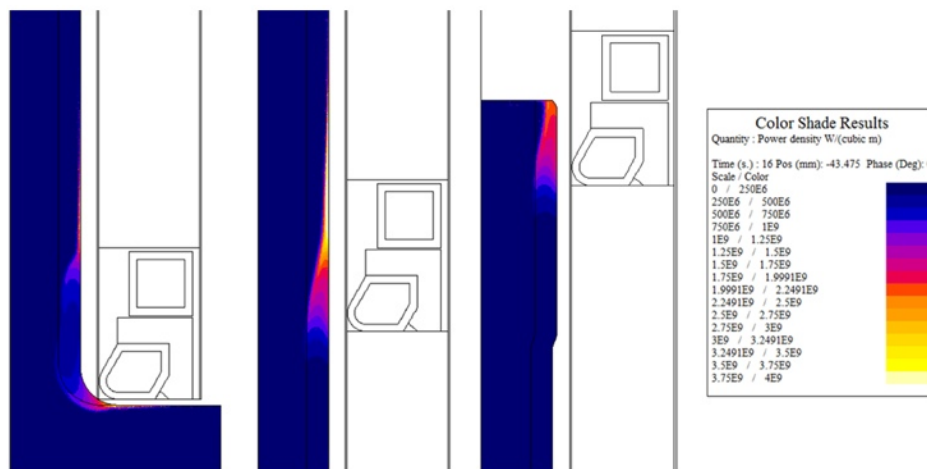

Figure 3: Power density distribution in fillet area at end of dwell (left),
shaft (middle), and spline at end of heat (right).

The induction heating and spray quenching processes are briefly described in table 1. The

spray starts at the beginning of step 3. The gap between the inductor and the spray is approximately 25.4 mm. At the end of step 3, the power distribution inside the shaft is stabilized, and step 4 covers the shaft. Inductor delivers heat to the spline during step 5, and the power is turned off at the end of step 5 to avoid excessive heat to the edge of the spline, which is not hardened for high ductility. During step 6, the power of the inductor is off, but the spray is continuous to ensure a complete martensitic transformation.

Table 1. Induction heating and spray quench schedule.

Step No.	Time Period (s)	Inductor Speed (mm/s)	Spray Quench
1	9.00	0.00	No
2	1.50	15.00	No
3	6.00	8.00	Yes
4	99.00	8.00	Yes
5	14.65	8.00	Yes
6	60.00	8.00 (Power Off)	Yes

Different finite element meshing models are used between Flux 2D and DANTE due to different physics and accuracy requirements. A 3D single tooth finite element meshing is used in DANTE for thermal, phase transformation, and stress analyses. Fine surface elements are used to catch the thermal and stress gradients effectively in the surface. The power densities in the axle predicted by Flux 2D are mapped and imported into DANTE. The mapping process is implemented at every 0.5 second time interval, and the power between two power snapshots is linearly interpolated. The temperature distributions predicted by Flux 2D and DANTE at various times of the process are compared, and the accuracy is successfully validated.

STRESSES AND PHASE TRANSFORMATION MODELING USING DANTE
The first step of induction hardening process is a 9 second dwell allowing the heat focusing on the flange and the fillet region. In this step, the inductor stays still without spray quench. The temperature and austenite distributions at the end of this step are shown in Figures 4(a) and 4(b). Because austenite has low strength at elevated temperature, the hoop stress in the austenitized zone is low. Due to the thermal expansion of the austenitized region, the region below the austenitized layer is under compression, and the center above the austenite zone is in tension as shown in Figure 4(c). In this model, the bottom of the OD flange is constraint in the axial direction to avoid rigid shifting, and the shaft expands axially with the heat into the part.
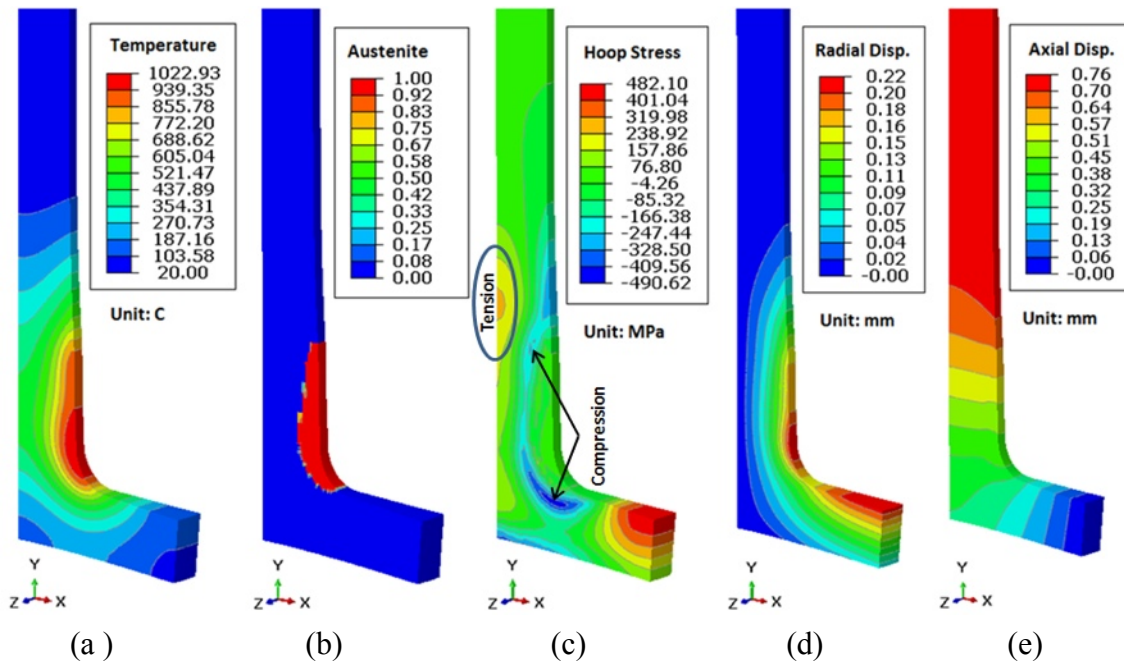
Figure 4: (a) Temperature, (b) austenite phase, (c) hoop stress, (d) radial displacement, and (e) axial displacement distributions at the end of 9 second dwell.

At the end of the first step of 9 second dwell, the inductor moves up with a speed of 15 mm/s for 1.5 seconds to avoid over heat the region above the fillet, then the speed drops down to 8mm/s with starting the spray quench until the end of the whole process. The power and temperature distributions of the shaft are stable for most portion of the process. The same power of heating is applied to the spline region, and the power is turned off at the end of the step 5 (at 130.15 second of the whole process), before the edge of the spline is austenitized. During the scanning process of the spline, the highest temperature predicted is about 1040° C, locating at the tip of the spline tooth. Ductile edge is preferred to avoid potential cracks during assemble and under service. Once the inductor is turned off, the heat conducts from the OD to the core, but there is not enough heat to increase the depth of the austenite layer. Figures 5(b) and 5(c) are the austenite and martensite distributions respectively, and the phase transformation from austenite to martensite follows the scanning spray quench process. Figure 5(d) is a snapshot of an in-process hoop stress distribution, which intuitively shows the effect of thermal gradient and phase transformation. Using the axial position as shown in Figure 5 as an example, the transformation from austenite to martensite is about completed, and compressive residual stresses are developed in the hardened layer due to the volume expansion along with martensitic transformation. The core at this axial position is still warm around 300° C, and further cooling of the core increases the magnitude of surface compression on the surface of the shaft. Figure 5(e) shows the in-process axial displacement distribution. At the lowest axial position in Figure 5, the temperature drops to room temperature, so the axial displacement below it is permanent distortion. The spline will go through cooling and martensite transformation process before reaching to room temperature and the axial displacement of the whole axle will decrease from the current snapshot.
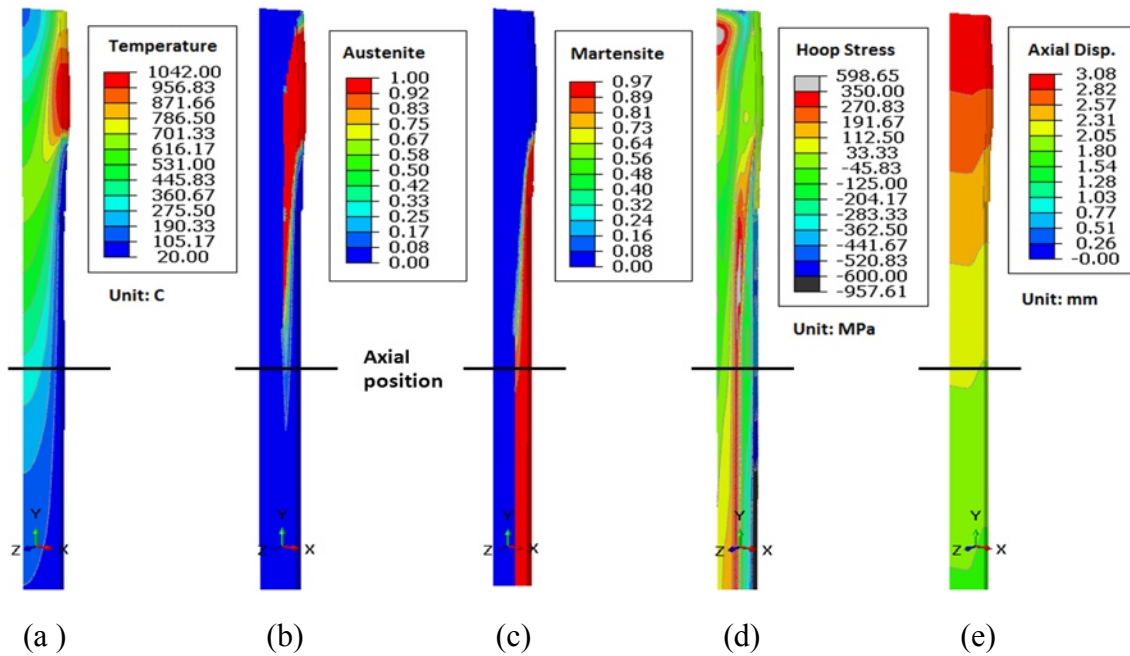
Figure 5: (a) Temperature, (b) austenite phase, (c) martensite, (d) hoop stress, and (e) axial displacement distributions at the end of heating process (130.15 second).

The axial residual stress distribution of the whole axle before tempering is shown in Figure 6. Most portion of the long shaft has the same axial residual stress profile, so the shaft is truncated for improved view. The residual compression on the surface of the shaft is under high compression of about 950 MPa, which is mainly due to the aggressive spray and high cooling rate. Inside the hardened layer but away from the surface, the residual compression in the axial direction is about 350 MPa. The core of the shaft is under tension around 540 MPa. At locations close to the flange and the spline, the predicted residual tensile stresses at the core are much higher, and they are 820 MPa, and 700 MPa, respectively. High residual tension is required to balance the high residual compression in the hardened layer. The high tensile residual stress under the hardened case can be detrimental if the axle is under bending. Too high of residual tension at the case-core interface also hurts the fatigue performance under torsion load. With mild spray and slower cooling rate, the magnitude of the residual stresses will be reduced. The spray quench process can be optimized based on the loading conditions of the axle under service.
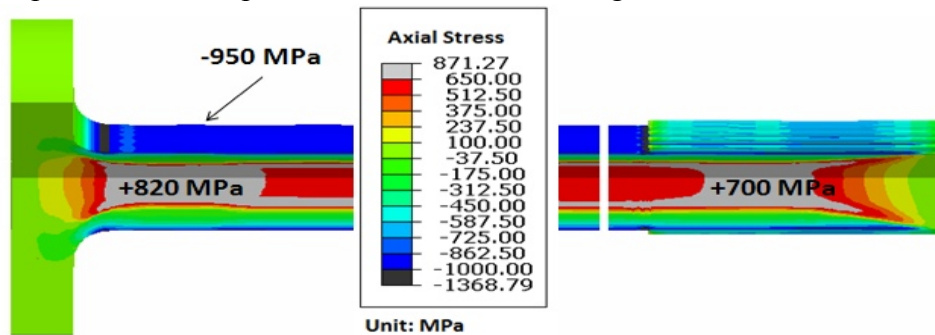

Figure 6: Axial residual stress distribution at the end of hardening process.

At the end of the induction hardening process, the temperature of the axle drops back to room temperature, the axial growth distribution is shown in Figure 7. Using the bottom of the flange as reference, the total growth in the axial direction is about 2.3 mm. The growth in the axial direction is mainly due to the material expansion of the hardened layer. The spray rate has significant effect on the axial growth. With mild spray, the growth in the axial direction is expected to reduce. Further studies of the spray rate effect on both residual stresses and axial distortion will be presented in following research works.
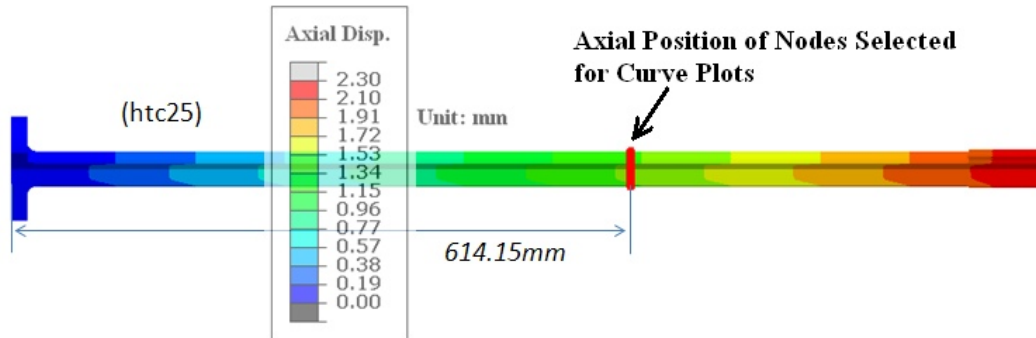

Figure 7: Axial displacement after induction hardening process.
(Showing selected points for curve plots)

(a)   (b)
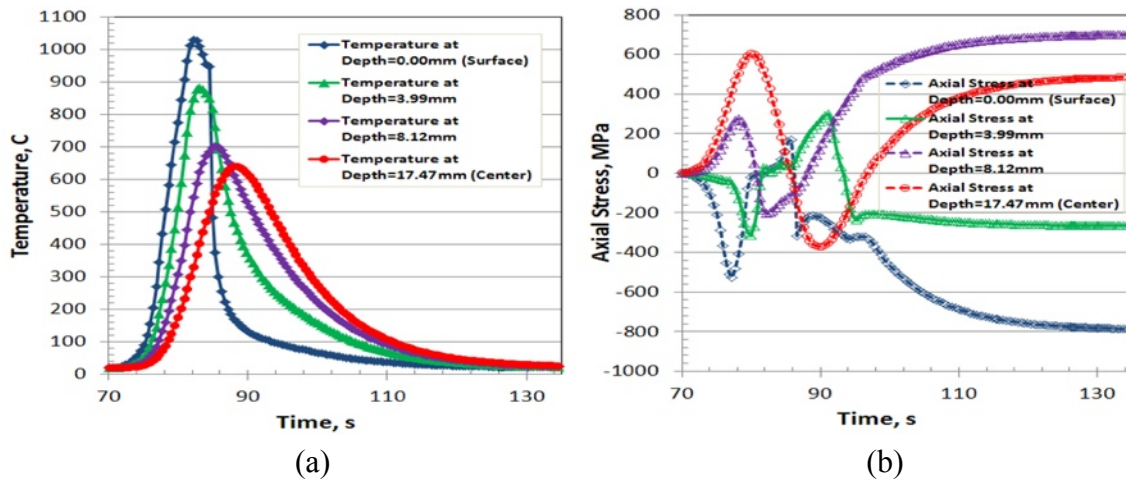
Figure 8: Curve plots of temperature and phase transformations of the four selected points.

To understand the relations of temperature, phase transformation, stress, and shape change, several points located at various depths from the surface of the shaft are selected for further post processing. The points selected are 614.15 mm from the bottom of the flange, as shown in Figure 7. The depth of the hardened layer on the shaft is 6.5 mm. The temperature and axial stress evolution at the four points during the scanning process are shown in Figure 8. Thermal gradients and phase transformations are the two main reasons to cause stress changing in the part.

CONCLUSIONS

The electromagnetic modelling using Flux and thermal-stress modelling using DANTE are

successfully coupled in this study. The power mapping process from Flux and DANTE is validated by directly comparing the temperature profiles predicted by the two packages. A relatively aggressive spray quenching process is used in this study. High surface compression on the surface of the shaft is predicted due to the high cooling rate. High tensile residual stresses are predicted at the case-core interface location of the as-quenched axle. The total length of the axle grows about 2.3 mm after induction hardening, and the shaft shrinks about 4 µm radially. It is known from past modelling experience that a milder spray rate will reduce the axial growth. The induction heating process parameters including frequency, power and scan speed, affect the temperature profile, which will significantly affect the residual stress distribution even without changing the case depth. The cooling rate also has a significant effect on the residual stress distributions. Influence of heating parameters and cooling rate on induction hardening results will be implemented and reported in future research studies. A tempering cycle will also be included. The simulation procedure developed in this study is promising for design optimization for failure prevention and service property prediction.

REFERENCES
[1] Goldstein, R., Nemkov, V., Jackowski, J. (2009) Virtual Prototyping of Induction Heat Treating. 25th ASM Heat Treating Society Conference.
[2] Ferguson, B., and Dowling, W., "Predictive Model and Methodology for Heat Treatment Distortion", NCMS Report #0383RE97, 1997
[3] Warke, V., Sisson, R., and Makhlouf, M., "FEA Model for Predicting the Response of Powder Metallurgy Steel Components to Heat Treatment", Mater. Sci. Eng., A, 2009, 518(1–2), pp. 7–15
[4] Bammann, D., et al., "Development of a Carburizing and Quenching Simulation Tool: A Material Model for Carburizing Steels Undergoing Phase Transformations", Proceedings of the 2nd International Conference on Quenching and the Control of Distortion, November (1996), pp. 367-375
[5] Ferguson, B.L., Freborg, A.M., Li, Z., "Probe Design to Characterize Heat Transfer during Quenching Process", Proceedings of 6th International Quenching and Control of Distortion Conference, Chicago, Illinois, September 9-13, 2012, pp. 792-801
[6] Nemkov, V., Goldstein, G., Jackowski, J. (2011). Stress and Distortion Evolution During Induction Case Hardening of Tube. 26th ASM Heat Treating Society Conference.
[7] Goldstein, R., Nemkov, V., Madeira, R., (2007). Optimizing Axle-Scan Hardening Inductors. Industrial Heating, December 2007.
[8] Li, Z., Ferguson, B., and Freborg, A., "Data Needs for Modeling Heat Treatment of Steel Parts", Proceedings of Materials Science & Technology Conference, 2004, pp. 219-226